Results in Physics 42 (2022) 105993

Contents lists available at ScienceDirect

Results in Physics

journal homepage: www.elsevier.com/locate/rinp

New soliton solutions for the conformal time derivative q-deformed physical model

Khalid K. Ali [a,*], Abdel-Haleem Abdel-Aty [b,c], Hichem Eleuch [d,e,f]

[a] Mathematics Department, Faculty of Science, Al-Azhar University, Nasr-City, Cairo, Egypt
[b] Department of Physics, College of Sciences, University of Bisha, P.O. Box 344, Bisha 61922, Saudi Arabia
[c] Physics Department, Faculty of Science, Al-Azhar University, Assiut, 71524, Egypt
[d] Department of Applied Physics and Astronomy, University of Sharjah, Sharjah, United Arab Emirates
[e] College of Arts and Sciences, Abu Dhabi University, Abu Dhabi, 59911, United Arab Emirates
[f] Institute for Quantum Science and Engineering, Texas A&M University, College Station, TX 77843, USA

ARTICLE INFO

Keywords:
q-deformed Sinh–Gordon equation
Conformal time derivative definition
Solitos solutions
The (G'/G)-expansion approach
The exponential cubic B-spline algorithm

ABSTRACT

In the present study, the conformal time derivative generalized q-deformed Sinh–Gordon equation is discussed analytically and numerically. This work is a continuation of a series of works presented recently, but we have developed the form of the equation in a way that all previous studies are a special case of it. We presented an extensive analytical and numerical study of the proposed equation using the (G'/G)-expansion approach and the exponential cubic B-spline algorithm respectively. Several figures are also provided to show the different solitons propagation patterns. The proposed model has opened up new options for describing physical systems that have lost their symmetry.

Introduction

Dynamical models in real life represent the foundation of many scientific fields such as physics, engineering, medical, and many applied sciences. These models employ nonlinear ordinary or partial differential equations to simulate a variety of real-world problems such as ocean engineering, optics, and the treatment of some diseases through the field of fluid mechanics, quantum mechanics, and others [1–5]. Nonlinearity has a significant impact on describing dynamics in quantum physics-governed microscopical systems [6,7]. Several researchers have investigated many partial differential equations in classical calculus that have substantial applications in various domains [8–11]. With the emergence of fractional calculus, the mathematical models were studied in a new form that contains the fractional derivatives in many papers as well such as [12–15]. With the presence of q-calculus, some researchers started thinking about putting all the relationships and laws in the classical and fractional calculus in q-calculus [16–18].

Calculus without bounds, or quantum calculus, is the same as conventional infinitesimal calculus but does not include the idea of boundaries. The terms "q-calculus" and "h-calculus" are differentiated, with h standing for Planck's constant and q for quantum [19].

The q-calculus has been created and used in many areas, including mathematical physics, the theory of relativity, and special functions (see for example [20–22]). The researchers began to expand the study of partial differential equations in q-calculus and they developed forms for the partial differential equations in q-calculus they were called q-deformed equations [23–25]. Working on such equations is a new direction taken by a few researchers. As we know that the Sin-Gordon equation has been studied by many researchers and also used under name of the Sin-Gordon method to find solutions to other differential equations [26–28].

The Sinh–Gordon equation [29]

$$\frac{\partial^2 \mathcal{L}}{\partial \chi^2} - \frac{\partial^2 \mathcal{L}}{\partial \tau^2} = [sinh(\mathcal{L})], \tag{1}$$

is widely used in physics and sciences. The sinh–Gordon Eq. (1) appears in integrable quantum field theory, kink dynamics, fluid dynamics, and in many other scientific applications. There is a growing interest in the study of the Sinh–Gordon equation, the double sinh–Gordon equation, and the triple sinh–Gordon equation. The sinh–Gordon equation also in (2 + 1) dimensions and (3 + 1)-dimensions have been studied from wazwaz [30]. The Eq. (1) can be generalized in the form:

$$\frac{\partial^2 \mathcal{L}}{\partial \chi^2} - \frac{\partial^2 \mathcal{L}}{\partial \tau^2} = [sinh_q(\mathcal{L}^\theta)]^l - \omega, \tag{2}$$

this equation was introduced and studied in this form for the first time in 2018 by Eleuch [23], then in 2022, Nauman et al. presented new optical soliton solutions for the same equation [24]. In the same year,

* Corresponding author.
E-mail addresses: khalidkaram2012@azhar.edu.eg (K.K. Ali), amabdelaty@ub.edu.sa (A.-H. Abdel-Aty), hichemeleuch@yahoo.fr (H. Eleuch).

https://doi.org/10.1016/j.rinp.2022.105993
Received 18 July 2022; Received in revised form 6 September 2022; Accepted 13 September 2022
Available online 21 September 2022

Ali and Abdel-Aty explored the analytical and numerical solutions of the same equation [25].

In this work, we presented a new form of the q-deformed Sinh–Gordon equation called The conformal time derivative generalized q-deformed Sinh-Gordon equation and studied it analytically and numerically.

The conformal time derivative generalized q-deformed Sinh–Gordon equation (Eleuch equation) is given by.

$$\frac{\partial^2 \mathcal{L}}{\partial \chi^2} - \frac{\partial^{2\beta} \mathcal{L}}{\partial \tau^{2\beta}} = [sinh_q(\mathcal{L}^\theta)]^l - \omega, \tag{3}$$

where θ, l are constants, $\beta \in (0,1]$ and $q \in (0,1)$. We get on the generalized q-deformed Sinh-Gordon equation from (3) at $\beta = 1$. Additionally, the Sinh-Gordon equation is given when $\beta = q = \theta = l = 1, \omega = 0$.

We investigate the soliton solutions of (3) using the (G'/G)- expansion approach. Furthermore, we use the exponential cubic B-spline algorithm to solve this equation numerically [31,32]. For this equation, we look at two cases.

The following is a breakdown of the structure of this paper: The second section introduces several q-calculus concepts and characteristics. The methodology of the analytical procedure is presented in the third section. The solutions are presented in the fourth part. The fifth section of the paper includes the numerical solutions. In the sixth section, we offer a few different variations of several solutions. In the last section, we present a conclusion to our work.

q-Calculus

The following are some fundamental definitions of the q-calculus: [16–18]

- Let a real parameter $0 < q < 1$, we define a q-real number $[s]_q$ by
  $$[s]_q = \frac{1-q^s}{1-q}, \ s \in \mathbb{R}.$$
- Differential of function is defined in the q-calculus as:
  $$d_q(\Lambda(\tau)) = \Lambda(q\tau) - \Lambda(\tau).$$
- The q-gamma function is described as follows:
  $$\Gamma_q(\tau) = \frac{S(q^\tau)}{(1-q)^{\tau-1}S(q)}, \ \tau \in \mathbb{R} - \{0,-1,-2,\dots\},$$
  where $S(q^\tau) = \frac{1}{(q^\tau;q)_\infty}$.
  Or, in other words,
  $$\Gamma_q(\tau) = \frac{1-q^{(\tau-1)}}{1-q^{\tau-1}},$$
  as well as satisfies $\Gamma_q(\tau+1) = [\tau]_q \Gamma_q(\tau)$.
- The formula for a function's q-derivative for f is
  $$(D_q\Lambda)(\tau) = \frac{d_q(\Lambda(\tau))}{d_q(\tau)} = \frac{\Lambda(\tau) - \Lambda(\tau q)}{\tau - q\tau}, \ (D_q\Lambda)(0) = \lim_{\tau\to\infty}(D_q\Lambda)(\tau).$$
- The $sinh_q$ is defined by:
  $$sinh_q(\tau) = \frac{e^\tau - qe^{-\tau}}{2}. \tag{4}$$
- The $cosh_q$ is defined by:
  $$cosh_q(\tau) = \frac{e^\tau + qe^{-\tau}}{2}. \tag{5}$$

The model's mathematical analysis

The traveling wave solution of (3) is determined using the transformation below

$$\mathcal{L}(\chi,\tau) = \upsilon(\varsigma), \tag{6}$$

where

$$\varsigma = \varrho\chi - \kappa\frac{\tau^\beta}{\beta}. \tag{7}$$

and κ denotes the speed of traveling wave.

The conformable derivative of order α is defined as

$$D_\tau^\beta \Lambda(\tau) = \lim_{\varepsilon\to 0}\frac{\Lambda(\tau+\varepsilon\tau^{1-\beta}) - \Lambda(\tau)}{\varepsilon},$$

for all $\tau > 0$, $\beta \in (0,1]$.

Using (6) and (7), then (3) becomes,

$$\left(\varrho^2 - \kappa^2\right)\upsilon''(\varsigma) + \varsigma - [\sinh_q(\upsilon(\varsigma)^\theta)]^l = 0. \tag{8}$$

Now consider two instances for (8).

- **Case one:** Suppose $l = \theta = 1, \omega = 0$.

Then, (8) can be written as:

$$\left(\varrho^2 - \kappa^2\right)\upsilon''(\varsigma) - \sinh_q(\upsilon(\varsigma)) = 0. \tag{9}$$

we can multiply both sides of (9) by $\upsilon'(\varsigma)$ and then integrate to obtain the equation shown below.

$$\frac{1}{2}\left(\varrho^2 - \kappa^2\right)(\upsilon'(\varsigma))^2 - \cosh_q(\upsilon(\varsigma)) - M_1 = 0, \tag{10}$$

where M_1 is the integration constant.

Let

$$\upsilon(\varsigma) = ln(u(\varsigma)). \tag{11}$$

By substituting from (11) into (10) with (5), thus, (10) becomes,

$$\left(\kappa^2 - \varrho^2\right)u'^2(\varsigma) + 2M_1u^2(\varsigma) + qu(\varsigma) + u^3(\varsigma) = 0. \tag{12}$$

Thus, we can resolve (12) and for the first case, we can determine the solution of (3) from (6) and (11).

- **Case two:** Suppose $\theta = 1, l = 2, \omega = -\frac{q}{2}$.

In this case, (8) can be expressed as:

$$\left(\varrho^2 - \kappa^2\right)\upsilon''(\varsigma) - \left(\sinh_q(\upsilon(\varsigma))\right)^2 - \frac{q}{2} = 0. \tag{13}$$

After simplify (13) we get

$$\left(\varrho^2 - \kappa^2\right)\upsilon''(\varsigma) - \frac{1}{2}\cosh_{q^2}(2\upsilon(\varsigma)) = 0. \tag{14}$$

Let

$$\upsilon(\varsigma) = \frac{1}{2}ln(u(\varsigma)). \tag{15}$$

Thus, (15) becomes,

$$2\left(\varrho^2 - \kappa^2\right)u'^2(\varsigma) - 2\left(\varrho^2 - \kappa^2\right)u(\varsigma)u''(\varsigma) + q^2u(\varsigma) + u^3(\varsigma) = 0. \tag{16}$$

As a result, we can solve (16) using a method described in the next section, so we can get the solution of (3) by using (15) and (6).

The strategy of the (G'/G)-expansion approach

Form the governing equation as follows:

$$F(\mathcal{L}, \mathcal{L}_{\chi\chi}, \mathcal{L}_{\tau\tau}, \dots) = 0, \tag{17}$$

where F is a polynomial in the set of all of $\mathcal{L} = \mathcal{L}(\chi,\tau)$ and its derivatives. To convert (17) to an ordinary differential equation, use a traveling wave transformation (6):

$$H(\upsilon, \upsilon'', \dots) = 0. \tag{18}$$

The (G'/G)-expansion method's key steps are:

Step 1: Assume that the exact solutions to (18) can be represented as:

$$\upsilon(\varsigma) = \sum_{i=0}^{N} B_i\left(\frac{G'}{G}\right)^i, \tag{19}$$

where $G = G(\varsigma)$ satisfies the second order linear ODE as follows:

$$G''(\varsigma) + \sigma G'(\varsigma) + \nu G(\varsigma) = 0, \tag{20}$$

where $B_i (i = 0, 1, 2, \ldots, N), B_N \neq 0, \sigma$ and ν, are constants to be calculated.

Step 2: The highest order derivative term in (8) is balanced with the highest power nonlinear term in (8) to produce the positive integer N in (19).

Step 3: We find three different families of (20) traveling wave solutions:

Family 1: Hyperbolic function solutions, when $\sigma^2 - 4\nu > 0$,

$$\frac{G'}{G} = \frac{-\sigma}{2} + \frac{1}{2}\sqrt{\sigma^2 - 4\nu}\frac{g_1 \sinh \frac{1}{2}\sqrt{\sigma^2 - 4\nu}\varsigma + g_2 \cosh \frac{1}{2}\sqrt{\sigma^2 - 4\nu}\varsigma}{g_1 \cosh \frac{1}{2}\sqrt{\sigma^2 - 4\nu}\varsigma + g_2 \sinh \frac{1}{2}\sqrt{\sigma^2 - 4\nu}\varsigma}. \tag{21}$$

Family 2: Trigonometric function solutions, when $\sigma^2 - 4\nu < 0$,

$$\frac{G'}{G} = \frac{-\sigma}{2} + \frac{1}{2}\sqrt{4\nu - \sigma^2}\frac{-g_1 \sin \frac{1}{2}\sqrt{4\nu - \sigma^2}\varsigma + g_2 \cos \frac{1}{2}\sqrt{4\nu - \sigma^2}\varsigma}{g_1 \cos \frac{1}{2}\sqrt{4\nu - \sigma^2}\varsigma + g_2 \sin \frac{1}{2}\sqrt{4\nu - \sigma^2}\varsigma}. \tag{22}$$

Family 3: Rational function solutions, when $\sigma^2 - 4\nu = 0$,

$$\frac{G'}{G} = \frac{-\sigma}{2} + \frac{g_2}{g_1 + g_2\varsigma}. \tag{23}$$

Step 4: By substituting (19) for (18) and using (20) to collect all terms with the same power of $(\frac{G'}{G})$ and then equating each coefficient to zero, a system of algebraic equations in $B_i, \sigma, \nu, \varrho, \kappa, M_1$ is obtained, which may be solved using the Mathematica program.

The model's mathematical solutions

The (G'/G)-expansion strategy is used in this section to determine the analytic solution to the two cases imposed for the problem (3)

- **The analytical solution of case one at $l = \theta = 1, \omega = 0$:**

Applying the balance principle in (12) between u'^2 and u^3 we get $2N+2 = 3N \Rightarrow N = 2$. From (19), the solution of (12) can be presented as:

$$\upsilon(\varsigma) = \sum_{i=0}^{2} B_i \left(\frac{G'}{G}\right)^i. \tag{24}$$

We get the following system by substituting (24) for (12) and setting the coefficient of like power of $\left(\frac{G'}{G}\right)$ to zero:

$$-\varrho^2 B_1^2 \nu^2 + B_1^2\kappa^2\nu^2 + 2B_0^2 M_1 + B_0 q + B_0^3 = 0,$$

$$-2\varrho^2 B_1^2 \sigma\nu - 4\varrho^2 B_1 B_2 \nu^2 + 2B_1^2\kappa^2\sigma\nu + 4B_1 B_2\kappa^2\nu^2$$

$$+4B_0 B_1 M_1 + B_1 + q + 3B_0^2 B_1 = 0,$$

$$-\varrho^2 B_1^2\sigma^2 - 8\varrho^2 B_1 B_2\sigma\nu - 4\varrho^2 B_2^2\nu^2 - 2\varrho^2 B_1^2\nu + B_1^2\kappa^2\sigma^2$$

$$+8B_1 B_2\kappa^2\sigma\nu + 4B_2^2\kappa^2\nu^2 + 2B_1^2\kappa^2\nu + 2B_1^2 M_1 + 4B_0 B_2 M_1 + B_2 q$$

$$+3B_0 B_1^2 + 3B_0^2 B_2 = 0,$$

$$-4\varrho^2 B_2 B_1\sigma^2 - 8\varrho^2 B_2^2\sigma\nu - 2\varrho^2 B_1^2\sigma - 8\upsilon^2 B_2 B_1\nu + 4B_2 B_1\kappa^2\sigma^2$$

$$+8B_2^2\kappa^2\sigma\nu + 2B_1^2\kappa^2\sigma + 8B_2 B_1\kappa^2\nu + 4B_2 B_1 M_1 + B_1^3 + 6B_0 B_2 B_1 = 0,$$

$$-4\varrho^2 B_2^2\sigma^2 - 8\varrho^2 B_1 B_2\sigma - 8\varrho^2 B_2^2\nu - \varrho^2 B_1^2 + 4B_2^2\kappa^2\sigma^2$$

$$+8B_1 B_2\kappa^2\sigma + 8B_2^2\kappa^2\nu + B_1^2\kappa^2 + 2B_2^2 M_1$$

$$+3B_0 B_2^2 + 3B_1^2 B_2 = 0,$$

$$-8\varrho^2 B_2^2\sigma - 4\varrho^2 B_1 B_2 + 8B_2^2\kappa^2\sigma + 4B_1 B_2\kappa^2 + 3B_1 B_2^2 = 0,$$

$$-4\varrho^2 B_2^2 + 4B_2^2\kappa^2 + B_2^3 = 0.$$

We get the following set of solutions by using the Mathematica programme to solve the previous set of equations.

- **Class 1:**

$$B_0 = -\frac{\sigma^2\sqrt{q}}{\sqrt{(\sigma^2 - 4\nu)^2}}, \quad B_1 = -\frac{4\sigma\sqrt{q}}{\sqrt{(\sigma^2 - 4\nu)^2}}, \quad B_2 = -\frac{4\sqrt{q}}{\sqrt{(\sigma^2 - 4\nu)^2}},$$
$$\varrho = \mp\sqrt{\kappa^2 - \frac{\sqrt{q}}{\sqrt{(\sigma^2 - 4\nu)^2}}}, \quad M_1 = \frac{\sqrt{q}\,(\sigma^2 - 4\nu)}{\sqrt{(\sigma^2 - 4\nu)^2}}. \tag{25}$$

Substituting from (25) to (24) with (11), (6) and into (21) and (22) respectively, we get the solutions of (3) at $l = \theta = 1, \omega = 0$:

Family 1: Hyperbolic function solutions, when $\sigma^2 - 4\nu > 0$,

$$\mathcal{L}_{1,2}(\chi,\tau) = ln\Bigg(B_0 + B_1\left(\frac{-\sigma}{2} + \frac{1}{2}\sqrt{\sigma^2 - 4\nu}\frac{g_1 \sinh \frac{1}{2}\sqrt{\sigma^2 - 4\nu}\varsigma + g_2 \cosh \frac{1}{2}\sqrt{\sigma^2 - 4\nu}\varsigma}{g_1 \cosh \frac{1}{2}\sqrt{\sigma^2 - 4\nu}\varsigma + g_2 \sinh \frac{1}{2}\sqrt{\sigma^2 - 4\nu}\varsigma}\right) + B_2\left(\frac{-\sigma}{2} + \frac{1}{2}\sqrt{\sigma^2 - 4\nu}\frac{g_1 \sinh \frac{1}{2}\sqrt{\sigma^2 - 4\nu}\varsigma + g_2 \cosh \frac{1}{2}\sqrt{\sigma^2 - 4\nu}\varsigma}{g_1 \cosh \frac{1}{2}\sqrt{\sigma^2 - 4\nu}\varsigma + g_2 \sinh \frac{1}{2}\sqrt{\sigma^2 - 4\nu}\varsigma}\right)^2\Bigg). \tag{26}$$

Family 2: Trigonometric function solutions, when $\sigma^2 - 4\nu < 0$,

$$\mathcal{L}_{3,4}(\chi,\tau) = ln\Bigg(B_0 + B_1\left(\frac{-\sigma}{2} + \frac{1}{2}\sqrt{\sigma^2 - 4\nu}\frac{-g_1 \sin \frac{1}{2}\sqrt{\sigma^2 - 4\nu}\varsigma + g_2 \cos \frac{1}{2}\sqrt{\sigma^2 - 4\nu}\varsigma}{g_1 \cos \frac{1}{2}\sqrt{\sigma^2 - 4\nu}\varsigma + g_2 \sin \frac{1}{2}\sqrt{\sigma^2 - 4\nu}\varsigma}\right) + B_2\left(\frac{-\sigma}{2} + \frac{1}{2}\sqrt{\sigma^2 - 4\nu}\frac{-g_1 \sin \frac{1}{2}\sqrt{\sigma^2 - 4\nu}\varsigma + g_2 \cos \frac{1}{2}\sqrt{\sigma^2 - 4\nu}\varsigma}{g_1 \cos \frac{1}{2}\sqrt{\sigma^2 - 4\nu}\varsigma + g_2 \sin \frac{1}{2}\sqrt{\sigma^2 - 4\nu}\varsigma}\right)^2\Bigg). \tag{27}$$

- **Class 2:**

$$B_0 = \frac{\sigma^2\sqrt{q}}{\sqrt{(\sigma^2 - 4\nu)^2}}, \quad B_1 = \frac{4\sigma\sqrt{q}}{\sqrt{(\sigma^2 - 4\nu)^2}}, \quad B_2 = \frac{4\sqrt{q}}{\sqrt{(\sigma^2 - 4\nu)^2}},$$
$$\varrho = \mp\sqrt{\kappa^2 + \frac{\sqrt{q}}{\sqrt{(\sigma^2 - 4\nu)^2}}}, \quad M_1 = -\frac{\sqrt{q}\,(\sigma^2 - 4\nu)}{\sqrt{(\sigma^2 - 4\nu)^2}}. \tag{28}$$

Substituting from (28) to (24) with (11), (6) and into (21) and (22) respectively, we get the solutions of (3) at $l = \theta = 1, \omega = 0$:

Family 1: Hyperbolic function solutions, when $\sigma^2 - 4\nu > 0$,

$$\mathcal{L}_{5,6}(\chi,\tau) = ln\Bigg(B_0 + B_1\left(\frac{-\sigma}{2} + \frac{1}{2}\sqrt{\sigma^2 - 4\nu}\frac{g_1 \sinh \frac{1}{2}\sqrt{\sigma^2 - 4\nu}\varsigma + g_2 \cosh \frac{1}{2}\sqrt{\sigma^2 - 4\nu}\varsigma}{g_1 \cosh \frac{1}{2}\sqrt{\sigma^2 - 4\nu}\varsigma + g_2 \sinh \frac{1}{2}\sqrt{\sigma^2 - 4\nu}\varsigma}\right) + B_2\left(\frac{-\sigma}{2} + \frac{1}{2}\sqrt{\sigma^2 - 4\nu}\frac{g_1 \sinh \frac{1}{2}\sqrt{\sigma^2 - 4\nu}\varsigma + g_2 \cosh \frac{1}{2}\sqrt{\sigma^2 - 4\nu}\varsigma}{g_1 \cosh \frac{1}{2}\sqrt{\sigma^2 - 4\nu}\varsigma + g_2 \sinh \frac{1}{2}\sqrt{\sigma^2 - 4\nu}\varsigma}\right)^2\Bigg). \tag{29}$$

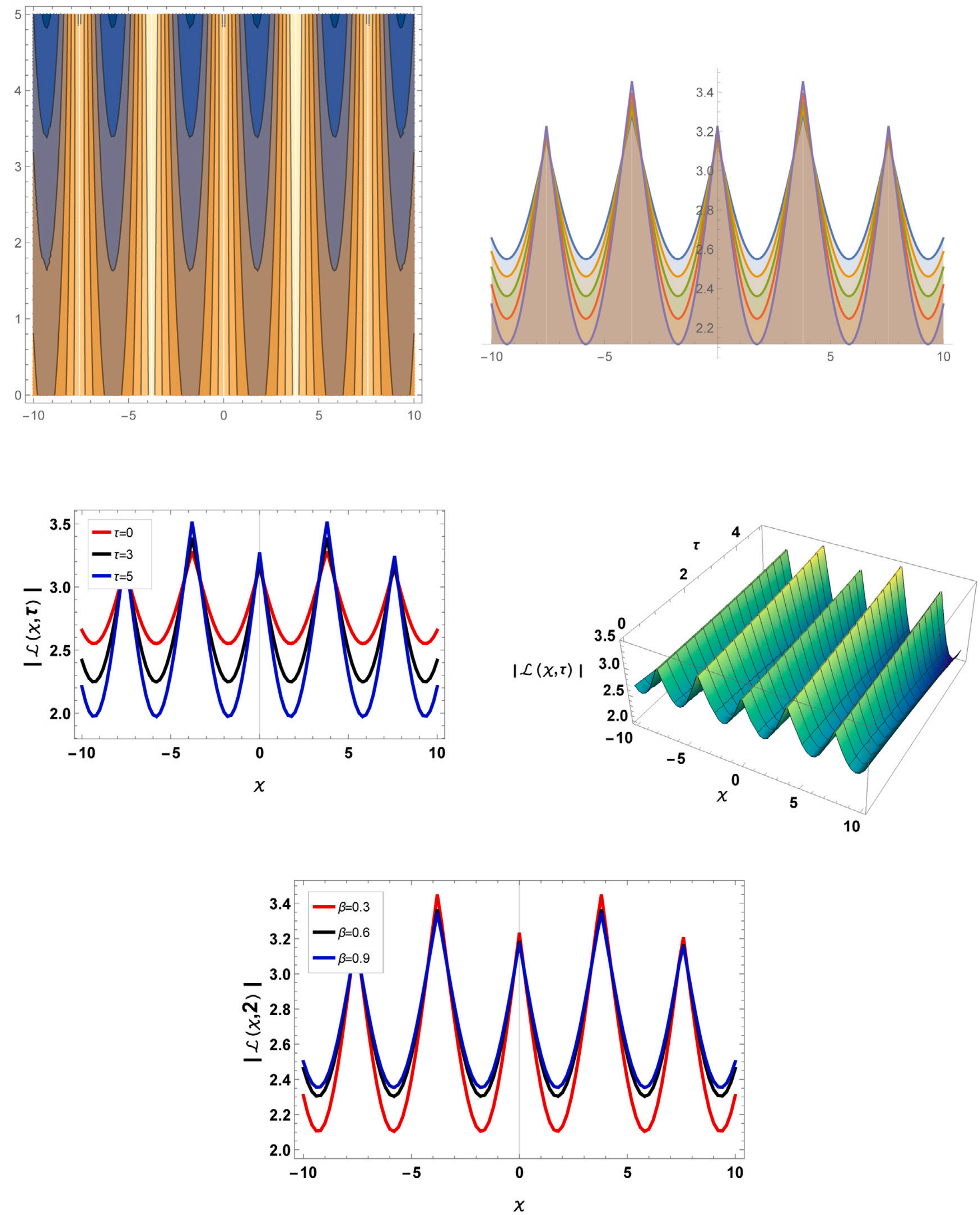

Fig. 1. Graph of (26) at $\nu = 0.01, \kappa = 0.3, \sigma = 0.5, \beta = 1, q = 0.5, g_1 = 1.1, g_2 = 1.5$.

Family 2: Trigonometric function solutions, when $\sigma^2 - 4\nu < 0$,

$$\mathcal{L}_{7,8}(\chi,\tau) = ln\Bigg(B_0 + B_1\left(\frac{-\sigma}{2} + \frac{1}{2}\sqrt{\sigma^2-4\nu}\,\frac{-g_1 \sin\frac{1}{2}\sqrt{\sigma^2-4\nu}\varsigma + g_2\cos\frac{1}{2}\sqrt{\sigma^2-4\nu}\varsigma}{g_1\cos\frac{1}{2}\sqrt{\sigma^2-4\nu}\varsigma + g_2\sin\frac{1}{2}\sqrt{\sigma^2-4\nu}\varsigma}\right) + B_2\left(\frac{-\sigma}{2} + \frac{1}{2}\sqrt{\sigma^2-4\nu}\,\frac{-g_1 \sin\frac{1}{2}\sqrt{\sigma^2-4\nu}\varsigma + g_2\cos\frac{1}{2}\sqrt{\sigma^2-4\nu}\varsigma}{g_1\cos\frac{1}{2}\sqrt{\sigma^2-4\nu}\varsigma + g_2\sin\frac{1}{2}\sqrt{\sigma^2-4\nu}\varsigma}\right)^2\Bigg). \tag{30}$$

- **The analytical solution of case two at** $l = 2, \theta = 1, \omega = -\frac{q}{2}$:

We get $2N + 2 = 3N \Rightarrow N = 2$ by using the balance principle in (16) between $\upsilon\upsilon''$ and υ^3. From (19), the solution of (12) can be presented as:

$$\upsilon(\varsigma) = \sum_{i=0}^{2} B_i\left(\frac{G'}{G}\right)^i. \tag{31}$$

We get the following system by substituting (31) into (16) and setting the coefficient of like power of $\left(\frac{G'}{G}\right)$ to zero:

$$-2\varrho^2 B_1 B_0 \sigma\nu - 4\varrho^2 B_2 B_0 \nu^2 + 2\varrho^2 B_1^2\nu^2 + 2B_1 B_0\kappa^2\sigma\nu$$
$$+4B_2 B_0\kappa^2\nu^2 - 2B_1^2\kappa^2\nu^2 + B_0 q^2 + B_0^3 = 0,$$
$$-2\varrho^2 B_0 B_1\sigma^2 + 2\varrho^2 B_1^2\sigma\nu - 12\varrho^2 B_0 B_2\sigma\nu + 4\varrho^2 B_1 B_2\nu^2 - 4\varrho^2 B_0 B_1\nu$$

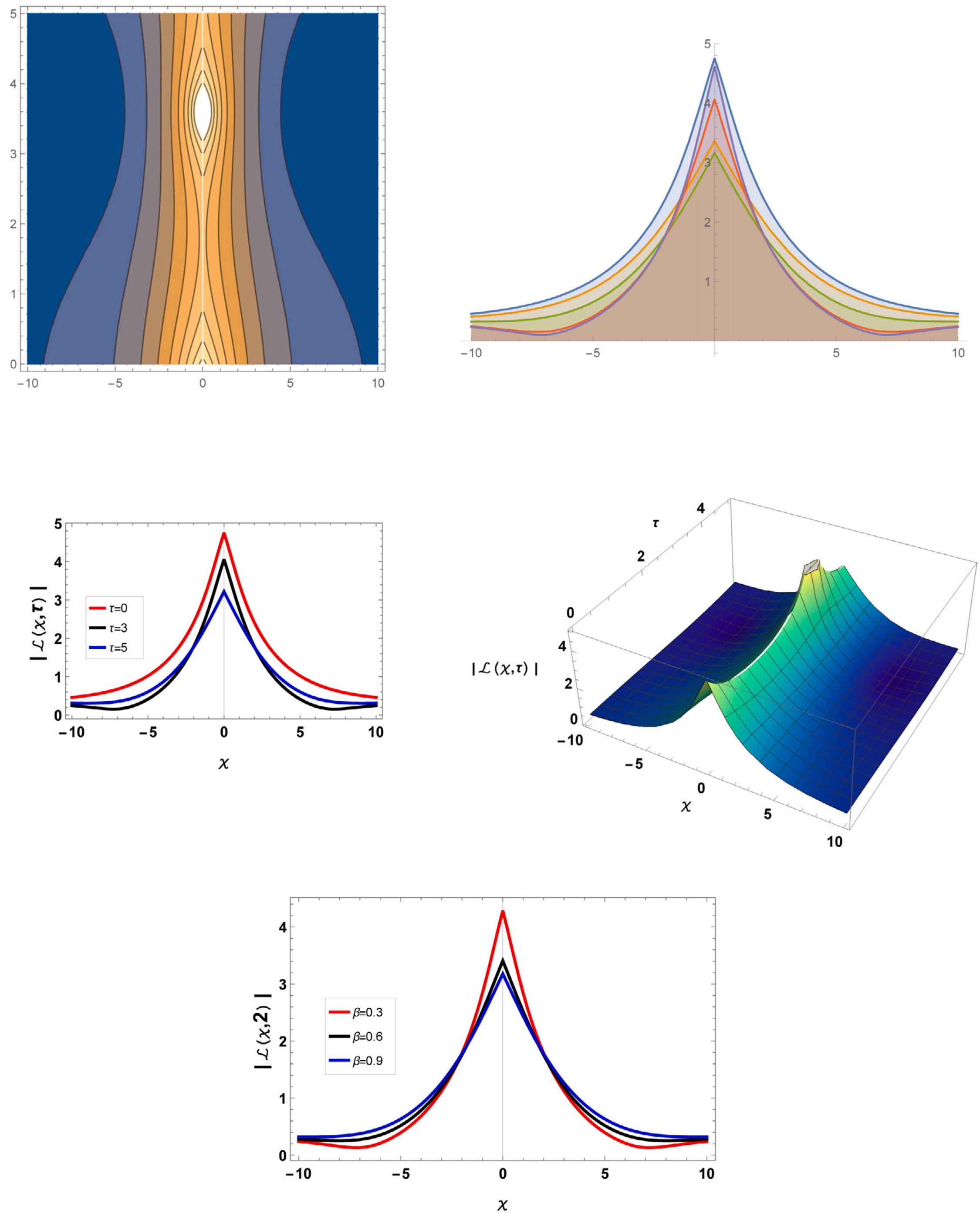

Fig. 2. Graph of (27) at $\nu = 0.3, \kappa = 0.7, \sigma = 0.1, \beta = 1, q = 0.5, g_1 = 0.1, g_2 = 0.2$.

$$+2B_0B_1\kappa^2\sigma^2 - 2B_1^2\kappa^2\sigma\nu + 12B_0B_2\kappa^2\sigma\nu - 4B_1B_2\kappa^2\nu^2$$

$$+4B_0B_1\kappa^2\nu + B_1 + q^2 + 3B_0^2B_1 = 0,$$

$$-8\varrho^2B_0B_2\sigma^2 + 2\varrho^2B_1B_2\sigma\nu - 6\varrho^2B_0B_1\sigma + 4\varrho^2B_2^2\nu^2 - 16a^2B_0B_2\nu$$

$$+8B_0B_2\kappa^2\sigma^2 - 2B_1B_2\kappa^2\sigma\nu + 6B_0B_1\kappa^2\sigma - 4B_2^2\kappa^2\nu^2$$

$$+16B_0B_2\kappa^2\nu + B_2q^2 + 3B_0B_1^2 + 3B_0^2B_2 = 0,$$

$$-2\varrho^2B_2B_1\sigma^2 + 4\varrho^2B_2^2\sigma\nu - 2\varrho^2B_1^2\sigma - 20\varrho^2B_0B_2\sigma - 4\varrho^2B_2B_1\nu$$

$$-4\varrho^2B_0B_1 + 2B_2B_1\kappa^2\sigma^2 - 4B_2^2\kappa^2\sigma\nu + 2B_1^2\kappa^2\sigma$$

$$+20B_0B_2\kappa^2\sigma + 4B_2B_1\kappa^2\nu + 4B_0B_1\kappa^2 + B_1^3 + 6B_0B_2B_1 = 0,$$

$$-10\varrho^2B_1B_2\sigma - 2\varrho^2B_1^2 - 12\varrho^2B_0B_2 + 10B_1B_2\kappa^2\sigma + 2B_1^2\kappa^2$$

$$+12B_0B_2\kappa^2 + 3B_0B_2^2 + 3B_1^2B_2 = 0,$$

$$-4\varrho^2B_2^2\sigma - 8\varrho^2B_1B_2 + 4B_2^2\kappa^2\sigma + 8B_1B_2\kappa^2 + 3B_1B_2^2 = 0,$$

$$-4\varrho^2B_2^2 + 4B_2^2\kappa^2 + B_2^3 = 0.$$

We get the following set of solutions by using the Mathematica programme to solve the previous set of equations.

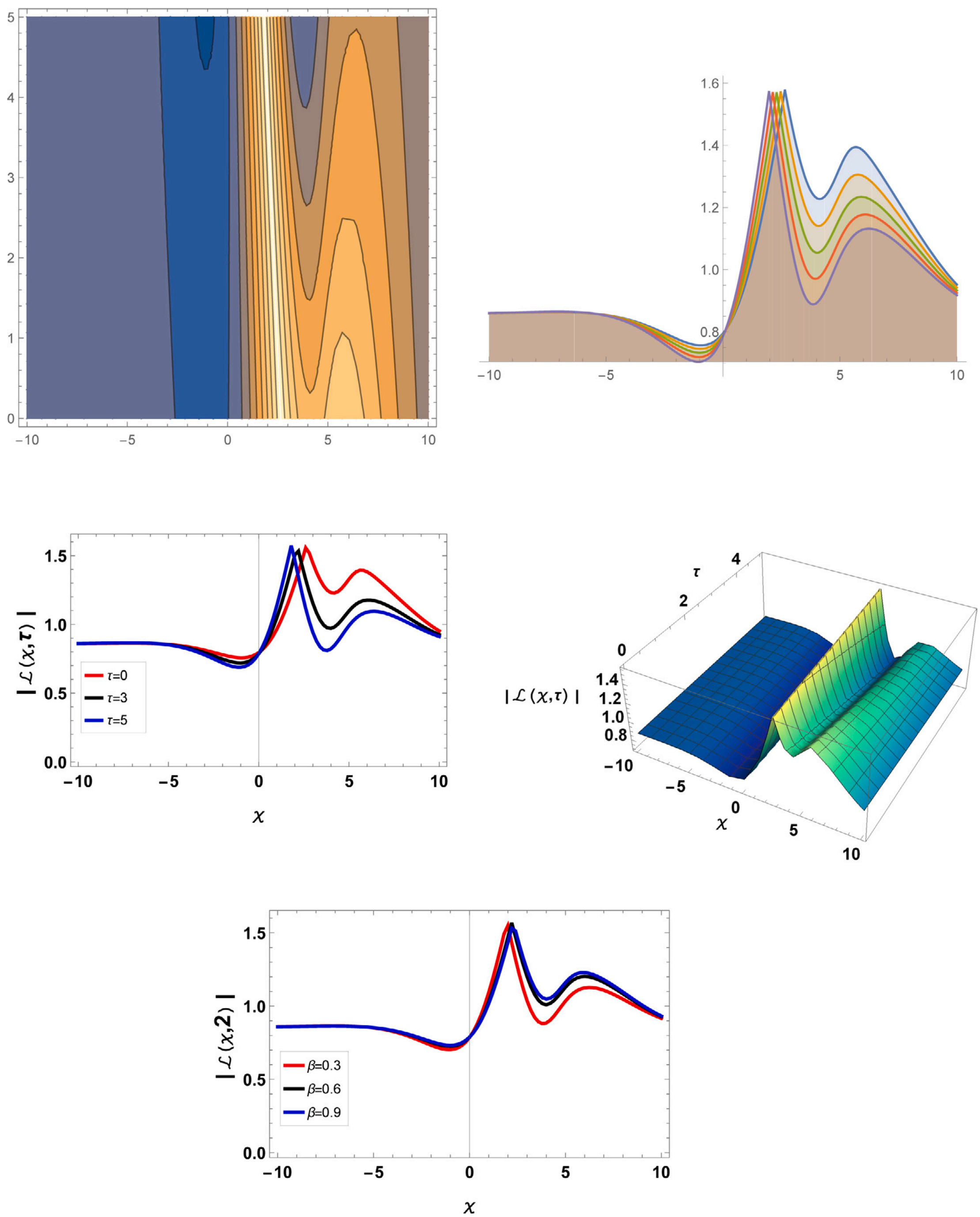

Fig. 3. Graph of (33) at $\nu = 0.01, \kappa = 0.5, \sigma = 0.3, \beta = 1, q = 0.5, g_1 = 1.2, g_2 = 1.5$.

- **Class 1:**

$$B_0 = \frac{\sigma^2 q^2}{\sqrt{-q^2\left(\sigma^2-4\nu\right)^2}},\quad B_1 = \frac{4\sigma q^2}{\sqrt{-q^2\left(\sigma^2-4\nu\right)^2}},$$
$$B_2 = \frac{4q^2}{\sqrt{-q^2\left(\sigma^2-4\nu\right)^2}},\quad \varrho = \mp\sqrt{\kappa^2 + \frac{q^2}{\sqrt{-q^2\left(\sigma^2-4\nu\right)^2}}}. \tag{32}$$

Substituting from (32) to (31) with (15), (6) and into (21) and (22) respectively, we get the solutions of (3) at $l = 2, \theta = 1, \omega = -\frac{q}{2}$:

Family 1: Hyperbolic function solutions, when $\sigma^2 - 4\nu > 0$,

$$\mathcal{L}_{1,2}(\chi,\tau) = ln\Bigg(B_0 + B_1\left(\frac{-\sigma}{2} + \frac{1}{2}\sqrt{\sigma^2-4\nu}\,\frac{g_1\sinh\frac{1}{2}\sqrt{\sigma^2-4\nu}\varsigma + g_2\cosh\frac{1}{2}\sqrt{\sigma^2-4\nu}\varsigma}{g_1\cosh\frac{1}{2}\sqrt{\sigma^2-4\nu}\varsigma + g_2\sinh\frac{1}{2}\sqrt{\sigma^2-4\nu}\varsigma}\right) + B_2\left(\frac{-\sigma}{2} + \frac{1}{2}\sqrt{\sigma^2-4\nu}\,\frac{g_1\sinh\frac{1}{2}\sqrt{\sigma^2-4\nu}\varsigma + g_2\cosh\frac{1}{2}\sqrt{\sigma^2-4\nu}\varsigma}{g_1\cosh\frac{1}{2}\sqrt{\sigma^2-4\nu}\varsigma + g_2\sinh\frac{1}{2}\sqrt{\sigma^2-4\nu}\varsigma}\right)^2\Bigg). \tag{33}$$

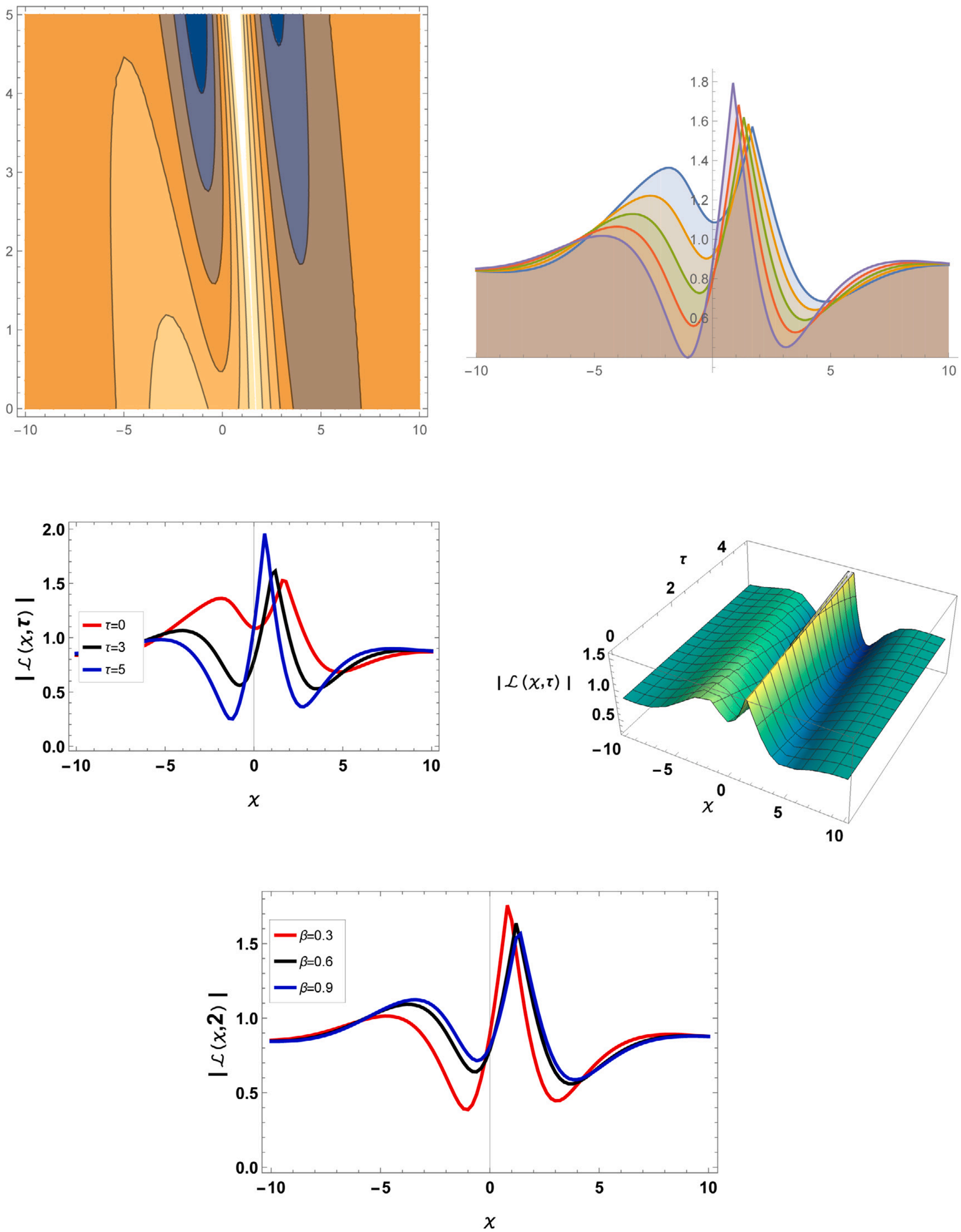

Fig. 4. Graph of (34) at $\nu = 0.2, \kappa = 0.3, \sigma = 0.1, \beta = 1, q = 0.5, g_1 = 0.3, g_2 = 0.2$.

Family 2: Trigonometric function solutions, when $\sigma^2 - 4\nu < 0$,

$$\mathcal{L}_{3,4}(\chi,\tau) = ln\Bigg(B_0 + B_1\left(\frac{-\sigma}{2} + \frac{1}{2}\sqrt{\sigma^2 - 4\nu}\frac{-g_1 \sin\frac{1}{2}\sqrt{\sigma^2-4\nu}\varsigma + g_2 \cos\frac{1}{2}\sqrt{\sigma^2-4\nu}\varsigma}{g_1 \cos\frac{1}{2}\sqrt{\sigma^2-4\nu}\varsigma + g_2 \sin\frac{1}{2}\sqrt{\sigma^2-4\nu}\varsigma}\right) + B_2\left(\frac{-\sigma}{2} + \frac{1}{2}\sqrt{\sigma^2 - 4\nu}\frac{-g_1 \sin\frac{1}{2}\sqrt{\sigma^2-4\nu}\varsigma + g_2 \cos\frac{1}{2}\sqrt{\sigma^2-4\nu}\varsigma}{g_1 \cos\frac{1}{2}\sqrt{\sigma^2-4\nu}\varsigma + g_2 \sin\frac{1}{2}\sqrt{\sigma^2-4\nu}\varsigma}\right)^2 \Bigg). \tag{34}$$

• **Class 2:**

$$B_0 = -\frac{\sigma^2 q^2}{\sqrt{-q^2\left(\sigma^2-4\nu\right)^2}}, \quad B_1 = -\frac{4\sigma q^2}{\sqrt{-q^2\left(\sigma^2-4\nu\right)^2}},$$
$$B_2 = -\frac{4q^2}{\sqrt{-q^2\left(\sigma^2-4\nu\right)^2}}, \quad \varrho = \mp\sqrt{\kappa^2 - \frac{q^2}{\sqrt{-q^2\left(\sigma^2-4\nu\right)^2}}}. \tag{35}$$

Substituting from (35) to (31) with (15), (6) and into (21) and (22) respectively, we get the solutions of (3) at $l = 2, \theta = 1, \omega = -\frac{q}{2}$:

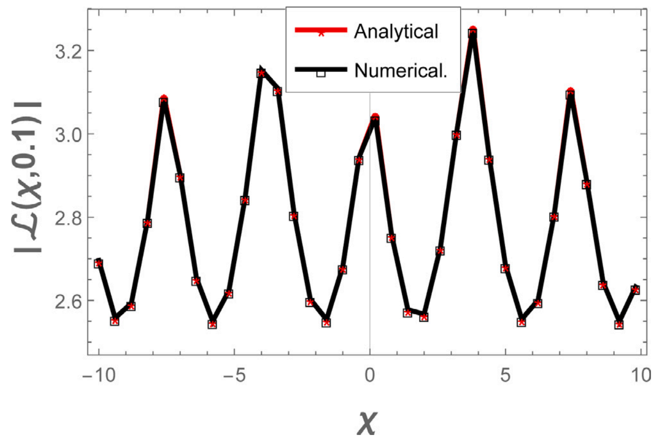

Fig. 5. Comparison between the numerical results of (3) with the analytical solution (26) at $\Delta\chi = 0.2, \Delta\tau = 0.01, \nu = 0.01, \kappa = 0.1, \sigma = 0.5, \rho = 0.0001, \beta = 1, q = 0.5, g_1 = 1.1, g_2 = 1.5$.

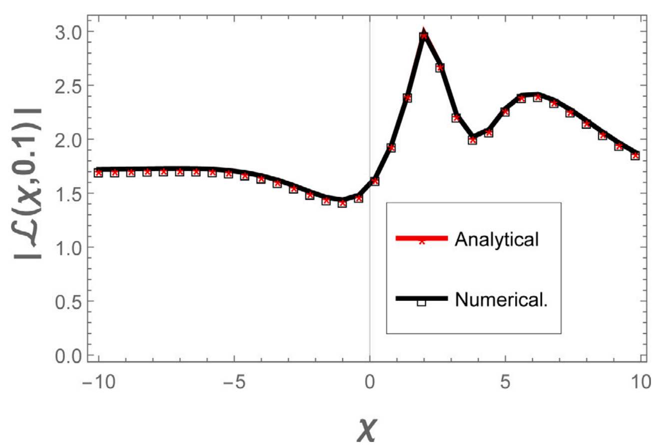

Fig. 6. Comparison between the numerical results of (3) with the analytical solution (33) at $\Delta\chi = 0.2, \Delta\tau = 0.01, \nu = 0.01, \kappa = 0.1, \sigma = 0.5, \rho = 0.0001, \beta = 1, q = 0.5, g_1 = 1.1, g_2 = 1.5$.

Family 1: Hyperbolic function solutions, when $\sigma^2 - 4\nu > 0$,

$$\mathcal{L}_{5,6}(\chi,\tau) = ln\Bigg(B_0 + B_1\left(\frac{-\sigma}{2} + \frac{1}{2}\sqrt{\sigma^2-4\nu}\,\frac{g_1\sinh\frac{1}{2}\sqrt{\sigma^2-4\nu}\varsigma + g_2\cosh\frac{1}{2}\sqrt{\sigma^2-4\nu}\varsigma}{g_1\cosh\frac{1}{2}\sqrt{\sigma^2-4\nu}\varsigma + g_2\sinh\frac{1}{2}\sqrt{\sigma^2-4\nu}\varsigma}\right) + B_2\left(\frac{-\sigma}{2} + \frac{1}{2}\sqrt{\sigma^2-4\nu}\,\frac{g_1\sinh\frac{1}{2}\sqrt{\sigma^2-4\nu}\varsigma + g_2\cosh\frac{1}{2}\sqrt{\sigma^2-4\nu}\varsigma}{g_1\cosh\frac{1}{2}\sqrt{\sigma^2-4\nu}\varsigma + g_2\sinh\frac{1}{2}\sqrt{\sigma^2-4\nu}\varsigma}\right)^2\Bigg). \tag{36}$$

Family 2: Trigonometric function solutions, when $\sigma^2 - 4\nu < 0$,

$$\mathcal{L}_{7,8}(\chi,\tau) = ln\Bigg(B_0 + B_1\left(\frac{-\sigma}{2} + \frac{1}{2}\sqrt{\sigma^2-4\nu}\,\frac{-g_1\sin\frac{1}{2}\sqrt{\sigma^2-4\nu}\varsigma + g_2\cos\frac{1}{2}\sqrt{\sigma^2-4\nu}\varsigma}{g_1\cos\frac{1}{2}\sqrt{\sigma^2-4\nu}\varsigma + g_2\sin\frac{1}{2}\sqrt{\sigma^2-4\nu}\varsigma}\right) + B_2\left(\frac{-\sigma}{2} + \frac{1}{2}\sqrt{\sigma^2-4\nu}\,\frac{-g_1\sin\frac{1}{2}\sqrt{\sigma^2-4\nu}\varsigma + g_2\cos\frac{1}{2}\sqrt{\sigma^2-4\nu}\varsigma}{g_1\cos\frac{1}{2}\sqrt{\sigma^2-4\nu}\varsigma + g_2\sin\frac{1}{2}\sqrt{\sigma^2-4\nu}\varsigma}\right)^2\Bigg). \tag{37}$$

Table 1
Comparison between the numerical results with the analytical solution.

χ	Numerical solution	Analytical solution	Absolute error
−10.0	2.69599	2.69604	6.96209 E-5
−8.0	2.88586	2.88586	4.19215 E-6
−6.0	2.56559	2.56558	3.82655 E-6
−4.0	3.15309	3.15309	4.22552 E-6
4.0	3.15309	3.15309	4.22552 E-6
6.0	2.56559	2.56558	3.82655 E-6
8.0	2.88586	2.88586	4.19215 E-6
10.0	2.69599	2.69604	6.96209 E-5

The numerical solution for the model

In this section, we use approximations for space χ and time τ derivatives as [31,32].

Now, we assume that $\mathcal{L}$ the exact solution at the grid point (χ_i, τ_n) and $\mathcal{L}^N$ is the numerical solution at the same point. Then the approximations for time χ derivative is

$$\mathcal{L}^N = a_1 c_{i+1,n} + c_{i,n} + a_1 c_{i-1,n}, \quad \mathcal{L}^N_{\chi\chi} = a_3 c_{i+1,n} - 2a_3 c_{i,n} + a_3 c_{i-1,n}. \tag{38}$$

where

$$a_1 = \frac{\xi - \Delta\chi\rho}{2(\alpha\Delta\chi\rho - \xi)}, \quad a_2 = \frac{(\alpha-1)\rho}{2(\alpha\Delta\chi\rho - \xi)}, \quad a_3 = \frac{\xi\rho^2}{2(\alpha\Delta\chi\rho - \xi)}.$$

From properties of the conformal derivative if $0 < \beta \leq 1$ and $\mathcal{L}$ be β differentiable at a point $\tau > 0$, then

$$\frac{\partial^\beta \mathcal{L}}{\partial\tau^\beta} = \tau^{1-\beta}\frac{\partial\mathcal{L}}{\partial\tau}. \tag{39}$$

The approximations for time τ derivative is

$$\mathcal{L}_\tau \simeq \frac{c_{i,n+1} - c_{i,n}}{\Delta\tau}. \tag{40}$$

From (39) and (40) we get

$$\frac{\partial^\beta \mathcal{L}}{\partial\tau^\beta} \simeq \tau^{1-\beta}\frac{c_{i,n+1} - c_{i,n}}{\Delta\tau}. \tag{41}$$

Substituting (38) and (41) into (3) we obtain the system of difference equations at $c_{i,n}$ as follows:

$$\begin{aligned} &a_3 c_{i+1,n} - 2a_3 c_{i,n} + a_3 c_{i-1,n} - \tau^{2-2\beta}\Bigg(\frac{(a_1 c_{i+1,n-1} + c_{i,n-1} + a_1 c_{i-1,n-1})}{(\Delta\tau)^2} \\ &+ \frac{(a_1 c_{i+1,n+1} + c_{i,n+1} + a_1 c_{i-1,n+1}) - 2(a_1 c_{i+1,n} + c_{i,n} + a_1 c_{i-1,n})}{(\Delta\tau)^2}\Bigg) \\ &- (1-\beta)\tau^{1-2\beta}\Bigg(\frac{-(a_1 c_{i+1,n-1} + c_{i,n-1} + a_1 c_{i-1,n-1})}{(2\Delta\tau)} \\ &+ \frac{(a_1 c_{i+1,n+1} + c_{i,n+1} + a_1 c_{i-1,n+1})}{2(\Delta\tau)}\Bigg) \\ &= [sinh_q((a_1 c_{i+1,n} + c_{i,n} + a_1 c_{i-1,n})^\theta)]^l - \omega. \end{aligned} \tag{42}$$

(42) can be solved by mathematica program to obtain the numerical results.

The numerical results

Now we will look at some numerical results for the q-deformed Sinh-Gordon equation in general. We also offer the numerical solution for two particular situations of the conformal time derivative generalized q-deformed Sinh-Gordon equation, as we examined the analytic solution for these two cases:

- **The numerical results for case one:** $l = \theta = 1, \omega = 0$

We compare the numerical results with the analytical solution (26) for (3) at $\Delta\chi = 0.2, \Delta\tau = 0.01, \nu = 0.01, \kappa = 0.1, \sigma = 0.5, \rho = 0.0001, \beta = 1, q = 0.5, g_1 = 1.1, g_2 = 1.5$ in Table 1 and Fig. 5.

Table 2
Comparison between the numerical results with the analytical solution.

χ	Numerical solution	Analytical solution	Absolute error
−10.0	1.72009	1.72009	1.37396 E-5
−8.0	1.72759	1.72760	1.39625 E-5
−6.0	1.72523	1.72524	1.47372 E-7
−4.0	1.66273	1.66273	1.65684 E-5
4.0	2.01908	2.01912	6.56488 E-5
6.0	2.42442	2.42454	1.55014 E-5
8.0	2.17196	2.17198	2.18673 E-5
10.0	1.85355	1.85354	1.36552 E-5

Table 3
Comparison between the numerical results with the analytical solution.

β	Numerical solution	Analytical solution	Absolute error
0.7	2.88479	2.88536	1.55415 E-3
0.8	2.88545	2.88563	4.99299 E-4
0.9	2.88573	2.88578	1.20010 E-4

Table 4
Comparison between the numerical results with the analytical solution.

β	Numerical solution	Analytical solution	Absolute error
0.7	2.16946	2.17101	1.54971 E-3
0.8	2.17101	2.17153	5.27333 E-4
0.9	2.17167	2.17182	1.50894 E-4

- **The numerical results for case two:** $l = 2, \theta = 1, \omega = -\frac{q}{2}$

In Table 2 and Fig. 6 we introduce comparison between the numerical results with the analytical solution (33) for (3) at $\Delta\chi = 0.2, \Delta\tau = 0.01, \nu = 0.01, \kappa = 0.1, \sigma = 0.5, \rho = 0.0001, \beta = 1, q = 0.5, g_1 = 1.1, g_2 = 1.5$.

We compare the numerical findings with the analytical solution (26) at $\Delta\chi = 0.2, \Delta\tau = 0.01, \nu = 0.01, \kappa = 0.1, \sigma = 0.5, \rho = 0.0001, q = 0.5, g_1 = 1.1, g_2 = 1.5, \chi = 8, \tau = 0.1$ with different values of β in Table 3.

In Table 4 we introduce comparison between the numerical results with the analytical solution (33) at $\Delta\chi = 0.2, \Delta\tau = 0.01, \nu = 0.01, \kappa = 0.1, \sigma = 0.5, \rho = 0.0001, q = 0.5, g_1 = 1.1, g_2 = 1.5, \chi = 8, \tau = 0.1$ with different values of β.

Graphical illustrations

Here, we show some two-dimensional and three-dimensional figures to clarify the solutions we presented. Figs. 1–6 depict some of the analytical and numerical solutions. In Fig. 1, we use our method to introduce the graph of (26) at $\nu = 0.01, \kappa = 0.3, \sigma = 0.5, \beta = 1, q = 0.5, g_1 = 1.1, g_2 = 1.5$, We notice in this figure that, the wave moves, retaining its shape and properties. It shifts down as time evolves. As time is fixed and β values change, the wave shifts up. In addition, Fig. 2 shows the graph of (27) $\nu = 0.3, \kappa = 0.7, \sigma = 0.1, \beta = 1, q = 0.5, g_1 = 0.1, g_2 = 0.2$, we notice in this figure that the wave moves, retaining its shape and properties. It shifts down as time evolves. As time is fixed and β values change, the wave shifts down. In addition, Fig. 3 shows the graph of (33) at $\nu = 0.01, \kappa = 0.5, \sigma = 0.3, \beta = 1, q = 0.5, g_1 = 1.2, g_2 = 1.5$, we notice in this figure that the wave moves, retaining its shape and properties shifts to left, as the time evolves. As time is fixed and β values change, the wave moves to the right. Fig. 4 shows the graph of (34) $\nu = 0.2, \kappa = 0.3, \sigma = 0.1, \beta = 1, q = 0.5, g_1 = 0.3, g_2 = 0.2$, we notice in this figure that the wave moves, retaining its shape and properties. It shifts left as time evolves. As time is fixed and β values change, the wave moves to the right. In addition, we compare the numerical results of (3) with the analytical solution (26) at $\Delta\chi = 0.2, \Delta\tau = 0.01, \nu = 0.01, \kappa = 0.1, \sigma = 0.5, \rho = 0.0001, \beta = 1, q = 0.5, g_1 = 1.1, g_2 = 1.5$ in Fig. 5. Finally, Fig. 6 shows a comparison of the numerical findings of (3) with the analytical solution of (33) at $\Delta\chi = 0.2, \Delta\tau = 0.01, \nu = 0.01, \kappa = 0.1, \sigma = 0.5, \rho = 0.0001, \beta = 1, q = 0.5, g_1 = 1.1, g_2 = 1.5$. Figs. 5, 6, which illustrate that the methodologies utilized are valid, show how well the numerical and analytical solutions they produced matched each other.

Conclusion

In this paper, we have derived the soliton solutions of the (1+1) conformal time derivative generalized q-deformed Sinh-Gordon equation using the (G'/G)-expansion approach. We have the model and gave figures demonstrating the validity of the results we planned to achieve using the proposed approach. We also presented a comprehensive numerical analysis of this model using the extended cubic B-spline algorithm. Furthermore, the analytical and numerical solutions are compared. The proposed equation has opened up new ways for defining physical systems that have lost their symmetry.

Declaration of competing interest

The authors declare that they have no known competing financial interests or personal relationships that could have appeared to influence the work reported in this paper.

Data availability

No data was used for the research described in the article.

References

[1] Braun Martin, Golubitsky Martin. Differential equations and their applications. vol. 1, New York: Springer-Verlag; 1983.
[2] Sun H, Chang A, Zhang Y, Chen W. A review on variable-order fractional differential equations: mathematical foundations, physical models, numerical methods and applications. Fract Calc Appl Anal 2019;22:27–59.
[3] Shahzad Muhammad, Abdel-Aty Abdel-Haleem, Attia Raghda AM, Khoshnaw Sarbaz HA, Aldila Dipo, Ali Mehboob, et al. Dynamics models for identifying the key transmission parameters of the COVID-19 disease. Alex Eng J 2021;60(1):757–65.
[4] Abdel-Aty AH, Khater MMA, Baleanu D, et al. Oblique explicit wave solutions of the fractional biological population (BP) and equal width (EW) models. Adv Differ Equ 2020;2020:552.
[5] Khater Mostafa MA, Attia Raghda AM, Abdel-Aty Abdel-Haleem. Computational analysis of a nonlinear fractional emerging telecommunication model with higher–order dispersive cubic–quintic. Inf Sci Lett 2020;9:83–93.
[6] Yusuf A, Sulaiman TA, Mirzazadeh M, Hosseini K. M-truncated optical solitons to a nonlinear Schrodinger equation describing the pulse propagation through a two-mode optical fiber. Opt Quantum Electron 2021;53(10):1–17.
[7] Kilbas AA, Srivastava HM, Trujillo JJ. Theory and applications of fractional differential equations. Amsterdam: Elsevier; 2006.
[8] Durur H, Ilhan E, Bulut H. Novel complex wave solutions of the (2+1)-dimensional hyperbolic nonlinear Schrödinger equation. Fractal Fract 2020;4(3):41.
[9] Almusawa Hassan, Ali Khalid K, Wazwaz Abdul-Majid, Mehanna MS, Baleanu D, Osman MS. Protracted study on a real physical phenomenon generated by media inhomogeneities. Results Phys 2021;31:104933.
[10] Ali Khalid K, Mehanna MS. Traveling wave solutions and numerical solutions of Gilson-Pickering Equation. Results Phys 2021;28:104596.
[11] Ali Khalid K, Mehanna MS. Computational and analytical solutions to modified Zakharov-Kuznetsov model with stability analysis via efficient techniques. Opt Quantum Electron 2021;53:723.
[12] Zafar A, Ali Khalid K, Raheel M, Jafar N, Nisar KS. Soliton solutions to the DNA Peyrard–Bishop equation with beta-derivative via three distinctive approaches. Eur Phys J Plus 2020;135(9):726.
[13] Osman MS, Ali Khalid K. Optical soliton solutions of perturbing time-fractional nonlinear Schrödinger equations. Optik 2020;209:164589.
[14] Osman MS, Zafar A, Ali Khalid K, Razzaq W. Novel optical solitons to the perturbed Gerdjikov–Ivanov equation with truncated M-fractional conformable derivative. Optik 2020;222:165418.
[15] Raslan KR, EL-Danaf TS, Ali Khalid K. Exact solution of space-time fractional coupled EW and coupled MEW equations using modified Kudryashov method. Commun Theor Phys 2017;68(1):49–56.
[16] Kac Victor G, Cheung Pokman. Quantum calculus. 2002, p. 113.
[17] Kac Victor, Cheung Pokman. Quantum calculus. In: Universitext. Springer-Verlag; 2002.
[18] Agarwal Ravi P. Certain fractional q-integrals and q-derivatives. In: Mathematical Proceedings of the Cambridge Philosophical Society. vol. 66, Cambridge University Press; 1969.

[19] SI Brochure: The International System of Units (SI) (PDF). (9th ed.). International Bureau of Weights and Measures; 2019, p. 131.
[20] Butt Rabia Ilyas, Abdeljawad Thabet, Alqudah Manar A, Rehman Mujeebur. Ulam stability of caputo q-fractional delay difference equation: q-fractional gronwall inequality approach. J Inequal Appl 2019;2019(1):1–13.
[21] Jleli Mohamed, Mursaleen Mohammad, Samet Bessem. Q-integral equations of fractional orders. Electron J Differential Equations 2016;2016(17):1–14.
[22] Abdeljawad Thabet, Baleanu Dumitru. Caputo q-fractional initial value problems and a q-analogue mittag–leffler function. Commun Nonlinear Sci Numer Simul 2011;16(12):4682–8.
[23] Eleuch H. Some analytical solitary wave solutions for the generalized q-deformed Sinh–Gordon equation $\frac{\partial^2\theta}{\partial z\partial\varsigma}$. Hindawi Adv Math Phys 2018;5242757:1–7.
[24] Raza Nauman, Arshed Saima, Alrebdi HI, Abdel-Aty Abdel-Haleem, Eleuch H. Abundant new optical soliton solutions related to q-deformed Sinh–Gordon model using two innovative integration architectures. Results Phys 2022;35:105358.
[25] Ali Khalid K, Abdel-Aty Abdel-Haleem. An extensive analytical and numerical study of the generalized q -deformed Sinh-Gordon equation. J Ocean Eng Sci 2022. http://dx.doi.org/10.1016/j.joes.2022.05.034.
[26] Yel G, Kumar Ajay, Baskonus Haci Mehmet, İlhan Esin. On the complex mixed dark-bright wave distributions to some conformable nonlinear integrable models. Fractals 2022;30(1):2240018.
[27] Yan Li, Yel Gulnur, Baskonus Haci Mehmet, Bulut Hasan, Gao Wei. Newly developed analytical method and its applications of some mathematical models. Internat J Modern Phys B 2022;36(4):2250040.
[28] Chen Q, Baskonus HaciMehmet, Ilhan WE. Soliton theory and modulation instability analysis: The Ivancevic option pricing model in economy. Alex Eng J 2022;61(10):7843–51.
[29] Grauel A. Sinh-Gordon equation painlevé property and bäcklund transformation. Physica A 1985;132:557–68.
[30] Abdul-Majid W. One and two soliton solutions for the Sinh–Gordon equation in (1 + 1), (2 + 1) and (3 + 1) dimensions. Appl Math Lett 2012;25:2354–8.
[31] Raslan KR, EL-Danaf TS, Ali Khalid K. New numerical treatment for solving the KDV equation. J Abs Comput Math 2017;2(1):1–12.
[32] EL-Danaf TS, Raslan KR, Ali Khalid K. New Numerical treatment for the Generalized Regularized Long Wave Equation based on finite difference scheme. Int J Soft Comp Eng 2014;4:16–24.